SU5416 plus hypoxia but not selective VEGFR2 inhibition with cabozantinib plus hypoxia induces pulmonary hypertension in rats: potential role of BMPR2 signaling

Ravikumar Sitapara[1],*, Chuluunbaatar Sugarragchaa[2] and Lawrence S. Zisman[1],*

[1]Gossamer Bio, Inc., San Diego, CA, USA; [2]Pulmokine, Inc., Rensselaer, NY, USA

Abstract

SU5416 plus chronic hypoxia causes pulmonary arterial hypertension in rats and is assumed to occur through VEGFR2 inhibition. Cabozantinib is a far more potent VEGFR2 inhibitor than SU5416. Therefore, we hypothesized that cabozantinib plus hypoxia would induce severe pulmonary arterial hypertension in rats. Cell proliferation and pharmacokinetic studies were performed. Rats were given SU5416 or cabozantinib subcutaneously or via osmotic pump and kept hypoxic for three weeks. Right ventricular systolic pressure and hypertrophy were evaluated at days 14 and 28 following removal from hypoxia. Right ventricular fibrosis was evaluated with Picro-Sirius Red staining. Kinome inhibition profiles of SU5416 and cabozantinib were performed. Inhibitor binding constants of SU5416 and cabozantinib for BMPR2 were determined and Nanostring analyses of lung mRNA were performed. Cabozantinib was a more potent VEGFR inhibitor than SU5416 and had a longer half-life in rats. Cabozantinib subcutaneous plus hypoxia did not induce severe pulmonary arterial hypertension. Right ventricular systolic pressure at 14 and 28 days post-hypoxia was 36.8 ± 2.3 mmHg and 36.2 ± 3.4 mmHg, respectively, versus 27.5 ± 1.5 mmHg in normal controls. For cabozantinib given by osmotic pump during hypoxia, right ventricular systolic pressure was 40.0 ± 3.1 mmHg at 14 days and 27.9 ± 1.9 mmHg at 28 days post-hypoxia. SU5416 plus hypoxia induced severe pulmonary arterial hypertension (right ventricular systolic pressure 61.9 ± 6.1 mmHg and 64.9 ± 8.4 mmHg at 14 and 28 days post-hypoxia, respectively). Cabozantinib induced less right ventricular hypertrophy (right ventricular free wall weight/(left ventricular free wall weight + interventricular septum weight) at 14 days post-hypoxia compared to SU5416. Right ventricular fibrosis was more extensive in the SU5416 groups compared to the cabozantinib groups. SU5416 (but not cabozantinib) inhibited BMPR2. Nanostring analyses showed effects on pulmonary gene expression of BMP10 and VEGFR1 in the SU5416 28 days post-hypoxia group. In conclusion, selective VEGFR2 inhibition using cabozantinib plus hypoxia did not induce severe pulmonary arterial hypertension. Severe pulmonary arterial hypertension due to SU5416 plus hypoxia may be due to combined VEGFR2 and BMPR2 inhibition.

Introduction

SU5416 plus chronic hypoxia is known to cause pronounced pulmonary arterial hypertension (PAH) with angio-obliterative pulmonary arteriolar lesions in rodents.[1] This effect is assumed to be mediated primarily through vascular endothelial growth factor receptor (VEGF) receptor (VEGFR) inhibition.[2] It has been proposed that SU5416 plus hypoxia results in an initial wave of pulmonary arteriolar endothelial cell (EC) apoptosis followed by the proliferation of apoptosis-resistant ECs.[3,4] The model is notable

for the persistence of severe pulmonary hypertension and progressive angio-obliterative pulmonary arteriolar lesions after return to normoxia. The severity of pulmonary

---

hypertension and features reminiscent of human PAH have made this an attractive model for translational research and drug development in the field of PAH. Given the premise that SU5416 contributes to the development of PAH in this model by virtue of its ability to inhibit VEGFR, it stands to reason that other VEGFR inhibitors when combined with hypoxia in a manner similar to the induction protocol typically used for the SU5416 hypoxia model would also result in severe pulmonary hypertension on return to normoxia. There are several VEGFR inhibitors approved for the treatment of renal cell carcinoma, medullary thyroid carcinoma, and other cancers which respond to the anti-angiogenic effects of VEGFR inhibition. These include sunitinib, pazopanib, axitinib, vandetanib, and cabozantinib.[5–8] Pazopanib inhibits the three major isoforms of VEGFRs (VEGFR1, 2, and 3), as well of platelet derived growth factor receptors (PDGFRs) and cKit.[9] Axitinib is more potent than pazopanib against VEGFR1, 2, and 3, with an IC_{50} in the range of 0.1–0.3 nM, but also inhibits PDGFRs and cKit in the nanomolar range.[5] Vandetanib inhibits VEGFR2 as well as epidermal growth factor receptor (EGFR).[10] Cabozantinib is one of the more highly potent VEGFR2 kinase inhibitors available with a reported IC_{50} of 0.035 nM.[11] We, therefore, chose to study cabozantinib in more detail, and hypothesized that cabozantinib plus hypoxia would induce severe pulmonary hypertension in rats.

Methods

SU5416 was obtained from Proactive Molecular Research (Alachua, FL); cabozantinib was obtained from LC Laboratories (Woburn, MA).

In vitro VEGFR2 kinase assay, cell proliferation assays, and pharmacokinetic studies

In vitro VEGFR2 kinase assays, human umbilical vein endothelial cell (HUVEC) and MRC5 proliferation assays, and pharmacokinetic studies in Sprague Dawley rats were performed (Pharmaron, Beijing, China). The rats were administered either SU5416 20 mg/kg subcutaneous (SC),

cabozantinib 20 mg/kg SC, or cabozantinib 12 mg/kg via an Alzet pump (over seven days). Three rats were studied per group. Plasma samples were obtained at serial timepoints, and SU5416 or cabozantinib were assayed by LC/MSMS.

Model and treatment protocol

Male SD rats (Taconic Biosciences; Rensselaer, NY) were given SU5416 (20 mg/kg) or the highly selective VEGFR2 inhibitor cabozantinib (20 mg/kg) via SC injection or cabozantinib via Alzet osmotic pump at a rate of 17.8 μg/h (designed to deliver drug for a total of 14 days) for a total calculated dose of about 20 mg/kg, and housed in a hypoxia chamber at FiO_2 10% for three weeks. The study schema is shown in Fig. 1. In addition to control normal rats not administered SU5416, cabozantinib, or hypoxia, there were the following four groups: SU5416 followed by three weeks of hypoxia and two weeks of normoxia (SU5416H21/14), SU5416 followed by three weeks of hypoxia and four weeks of normoxia (SU5416H21/28), cabozantinib SC by single injection or Alzet pump with three weeks of hypoxia and two weeks of normoxia (CaboH21/14), and cabozantinib SC by single injection or Alzet pump with three weeks of hypoxia and four weeks of normoxia (CaboH21/28). Rats were housed with standard diet, water ad libitum, and 12-h light cycle. The study was approved by the Pulmokine IACUC and adhered to the NIH Guide for the care and use of vertebrate animals in research.

End of study procedures

At the end of the study, rats were sedated, intubated, and placed under general anesthesia with isoflurane. A sternotomy was performed, and right ventricular (RV) hemodynamics measured with a Scisense catheter. The rats were euthanized by exsanguination under general anesthesia. Lungs were harvested for histologic analyses. RV hemodynamics and RV hypertrophy (RVH) by Fulton's Index (RV/ (left ventricular (LV) + interventricular septum (IVS))) were evaluated at 14 and 28 days after the end of hypoxia exposure, corresponding to total days 35 and 49 of the protocol, respectively.
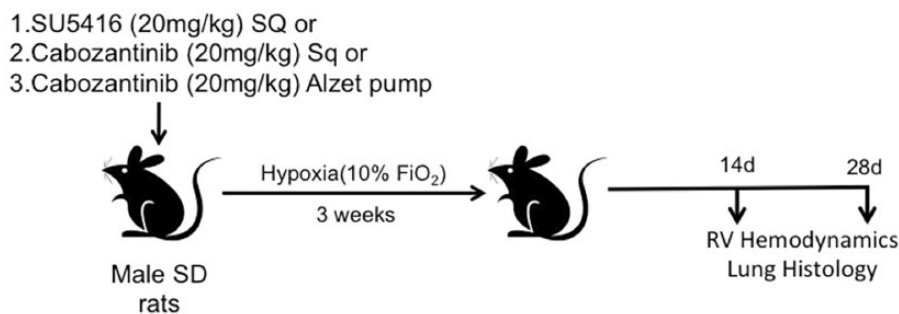

Fig. 1. Study schema. Male Sprague Dawley (SD) rats were given SU5416 20 mg/kg subcutaneously (SC), cabozantinib 20 mg/kg SC, or cabozantinib 17.8 μg/h by an Alzet osmotic minipump. Animals were placed in a hypoxia chamber at FiO_2 10% for three weeks and then returned to normoxia. End of study procedures were performed 14 or 28 days after removal from the hypoxia chamber.

Histomorphometric analysis

After removal of the heart and lungs, heparinized saline was infused under pressure through the main pulmonary artery. The heart was removed, and the RV free wall, IVS, and LV free wall were dissected and weighed. Buffered formalin (10%) was infused under pressure through both the pulmonary artery and the trachea. Morphometric analysis was performed on hematoxylin and eosin-stained formalin-fixed tissue sectioned at 8 μm. The media area and lumen area of pulmonary arterioles were measured with ImageJ software. Measurements were made on at least 20 pulmonary arterioles per section. The ratio of the lumen area to the total media area was determined. This ratio normalizes the variation in total pulmonary arteriole area. Picro-Sirius red staining of the right ventricles was performed to evaluate for presence of fibrosis (WAX-IT, Vancouver BC).

Kinome scan and BMPR2 assays

SU5416 (10,000 nM) and cabozantinib (10,000 nM) were screened for inhibitor activity against 468 human kinases using KINOMEscan™ Profiling (DiscoverX; San Diego, CA). Inhibitor binding constants (Kd) of SU5416 and cabozantinib for bone morphogenic protein receptor type 2 (BMPR2) were determined by KdELECT assay (DiscoverRx, San Diego, CA).

Nanostring analysis

RNA was extracted from 12 formalin fixed paraffin embedded (FFPE) lung samples. Isolated RNA was analyzed using the mouse PanCancer Immune Profiling Panel on the nCounter System (NanoString Technologies). Raw gene counts produced from the nCounter system were normalized and analyzed for differential gene expression by ROSALIND® (https://rosalind.onramp.bio/), with a HyperScale architecture developed by OnRamp BioInformatics, Inc. (San Diego, CA). The mouse PanCancer pathways panel was used with the addition of the following rat-specific probes: BMP9 (NM_001106096.1), BMP10 (NM_001031824.1), BMPR2 (XM_001065181.1), small mothers against decapentaplegic 5 (SMAD5) (NM_021692.1), VEGFR1 (NM_019306.1), and VEGFR2 (NM_013062.1).

Statistical analysis

Analysis of variance followed by the Bonferroni correction for multiple group comparisons, or Dunnett's test for comparison to a control group was used to evaluate differences between groups for the parameters of interest. For the Nanostring analyses, the Kruskal–Wallis test followed by Dunn's test for multiple comparisons was used. Significance was set at $p < 0.05$. Unless otherwise specified, data are presented as the mean $\pm$ SEM.

Results

In a VEGFR2 kinase assay, SU5416 was found to have an IC_{50} of 438.5 nM, whereas cabozantinib was found to have an IC_{50} of 9.0 nM. In a HUVEC proliferation assay, SU5416 showed an IC_{50} of 330 nM, whereas the cabozantinib IC_{50} was 4.9 nM. In an MRC5 proliferation assay (a fibroblast cell line), the SU5416 IC_{50} was 11,726 nM, whereas that for cabozantinib was 549 nM (Table 1). The results of the pharmacokinetic studies are shown in Table 2.

Selective inhibition of VEGFR2 using cabozantinib (SC injection) plus hypoxia did not induce severe PAH. Right ventricular systolic pressure (RVSP) measured at 14 and 28 days post-hypoxia were 36.8 ± 2.3 and 36.2 ± 3.4 mmHg, respectively, compared to 27.5 ± 1.5 mmHg in a normal control group. When cabozantinib was given at a continuous rate of 17.8 µg/h using an Alzet osmotic pump for 14 of the 21 days of hypoxia, RVSP was 40.0 ± 3.1 mmHg at 14 days and 27.9 ± 1.9 mmHg at 28 days after removal from hypoxia. Consistent with its known effect, SU5416 plus hypoxia exposure induced severe PAH (RVSP 61.9 ± 6.1 and 64.9 ± 8.4 mmHg at 14 and 28 days post removal from hypoxia, respectively) (Fig. 2).

Cabozantinib (via SC injection or Alzet osmotic pump) induced less RVH at 14 days post-hypoxia compared to SU5416 as measured by Fulton's Index: Cabo 0.36 ± 0.02 vs. SU5416 0.58 ± 0.02 ($p < 0.0001$). After 28 days, RVH was significantly increased in the SU5416 group compared to the control group ($p = 0.024$); there was no significant difference in RVH between the normal control group and the Cabo group at 28 days (Fig. 3). RVH appeared to decrease from day 14 to day 28 after removal from hypoxia in the SU5416 without a decrease in RV systolic pressure. Qualitatively, there was an increase in RV fibrosis at both days 14 and 28 after removal from hypoxia in the SU5416H groups compared to the CaboH groups (Fig. 3).

The lumen/media ratio of the pulmonary arterioles was significantly decreased in the SU5416/H animals compared to the cabozantinib/H groups (Fig. 4).

Table 1. IC_{50} (nM) values for in vitro VEGFR kinase assays.

Drug	VEGFR (nM)	HUVECs (nM)	MRC5 (nM)
SU5416	438.5	330	11,726
Cabozantinib	9	4.9	549

VEGFR: VEGF receptor.

Table 2. Results of the pharmacokinetic studies comparing SU5416 and cabozantinib.

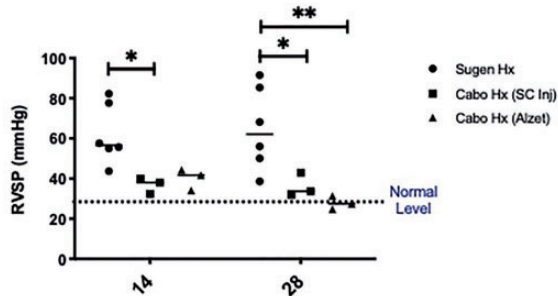| Drug	T1/2 (h)	Cmax (ng/ml)	AUClast (h × ng/ml)
SU5416 (20 mg/kg SC)	5 ± 4.7	4.97 ± 2.3	12.6 ± 2
Cabo (20 mg/kg SC)	25.7 ± 10.8	1617 ± 103	$27,537 \pm 1698$
Cabo (Alzet 12 mg/kg)	43 ± 8	238 ± 83	$16,772 \pm 3332$

Fig. 2. Right ventricular end systolic pressure (RVSP) is shown for the SU5416 hypoxia (SU5416H) group, the cabozantinib (Cabo) SC hypoxia group, and the Cabo administered via an Alzet pump hypoxia group. RVSP was significantly elevated by SU5416H on days 14 and 28 vs. normal controls or vs. Cabo groups. Normal control RVSP is represented by the dotted line based on data from healthy normal rats. $*p = 0.001$; $**p < 0.05$.

To understand potential off-target effects, KINOMEscan[TM] profiles against 468 human kinases were performed for SU5416 and cabozantinib. SU5416, but not cabozantinib, was found to be a potential inhibitor of BMPR2. The full kinome scan results are provided in supplementary files. SU5416 had a greater binding affinity for BMPR2, compared to cabozantinib. A KdELECT assay was performed to compare the Kd of SU5416 and cabozantinib for BMPR2. SU5416 had a Kd of 2.1 μM, whereas the cabozantinib Kd for BMPR2 was > 10 μM (Fig. 5).

The full Nanostring dataset is provided in the supplement. *BMP10* gene expression was significantly increased in the SU5416H21/24 group compared to the control group. A trend toward a similar increase was observed for BMP9 but this did not reach statistical significance. There were no statistically significant differences between
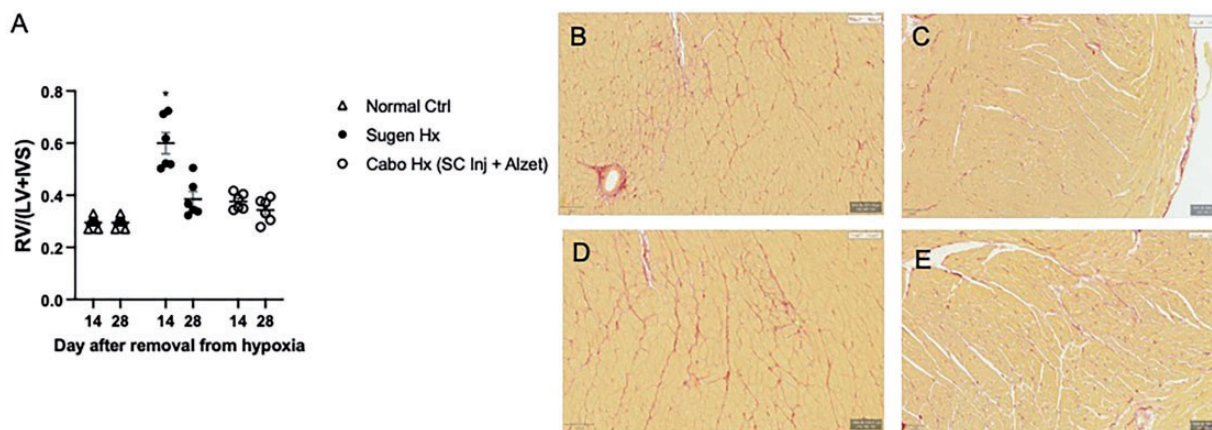

Fig. 3. Right ventricular hypertrophy (RVH) measured by Fulton's Index (RV/(LV + IVS)) is shown for normal controls, SU5416, Cabo (SC + Alzet groups) at 14 and 28 days. $*p < 0.0001$; $**p < 0.05$ (A). Representative images of Picro-Sirius stains of RVs are shown for SU5416H21/14 (B); CaboH21/14 (C); SU5416H21/28 (D) and CaboH21/28 (E). There is evidence of increased RV fibrosis in the SU5416H groups at both timepoints compared to the CaboH groups.
LV: left ventricular free wall weight; IVS: interventricular septum weight; RV: right ventricular free wall weight; SC: subcutaneous.
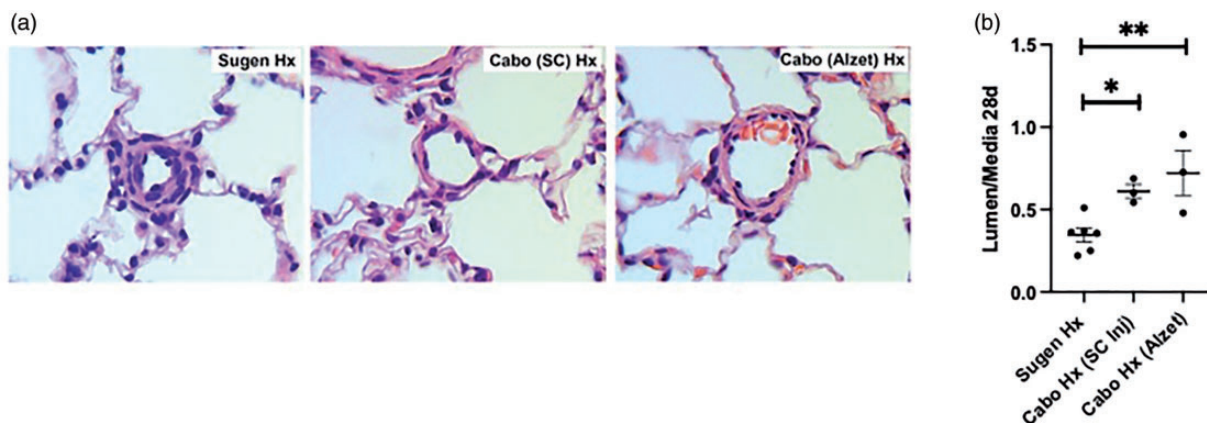

Fig. 4. Photomicrographs demonstrating medial thickening of a pulmonary arteriole in a SU5416/H rat, with less medial hypertrophy in a Cabo SC hypoxia-treated rat and Cabo Alzet hypoxia-treated rat (A); this difference was quantified by the lumen to media ratio (L/M) which was decreased in the SU5416/H group compared to the Cabo groups at day 28 (B); $*p = 0.047$ SU5416 vs. Cabo SC; $**p = 0.008$, SU5416 vs. Cabo Alzet group.
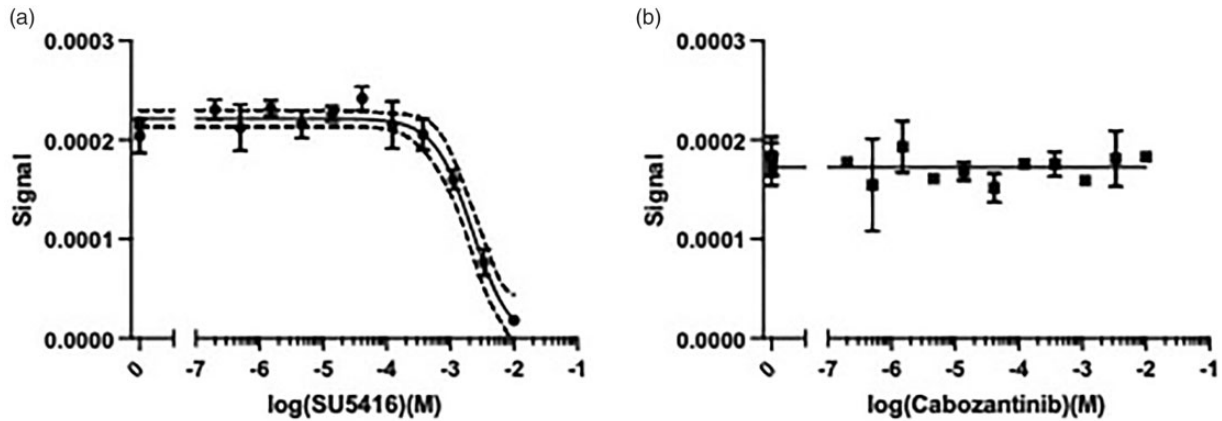
Fig. 5. BMPR2 KdELECT assay for SU5416 (a) and cabozantinib (b). The Kd for SU5416 was 2.1 μM. The Kd for cabozantinib was >10 μM.
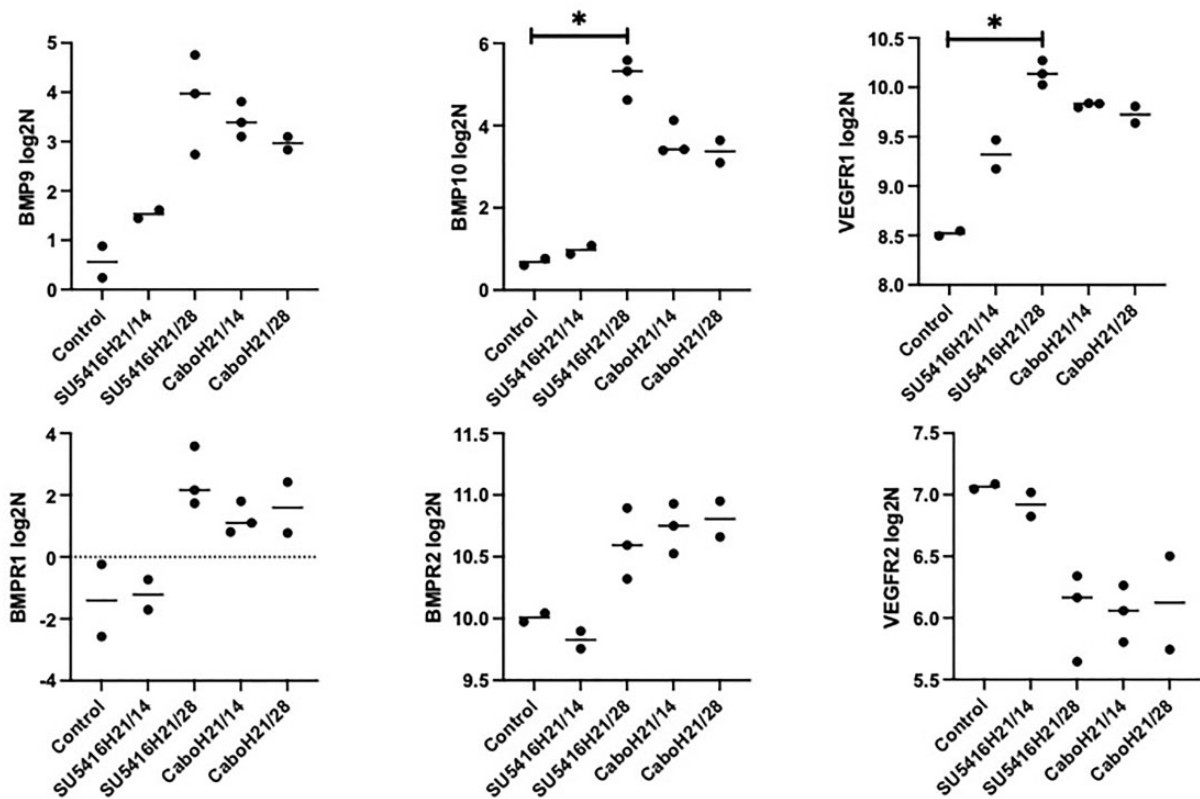

Fig. 6. Results of selected targets from Nanostring analyses are shown with individual data points and median values of log2 normalized expression levels for: BMP9, BMP10, BMPR1, BMPR2, VEGFR1, and VEGFR2. Compared to the control group, BMP10 and VEGFR1 were increased in the SU5416H21/28 group (*$p = 0.016$).

the groups at the timepoints studied for BMPR1, BMPR2, or VEGFR2 (Fig. 6). However, VEGFR1 and PDGFB expression were increased in the SU5416H21/28 group compared to the control group ($p = 0.0156$ and $p = 0.04$ respectively). No differences were found between the groups for SMAD1, SMAD2, SMAD3, or SMAD5. However, SMAD9 was increased in the CaboH21/14 group compared to the control group ($p = 0.02$). There were no significant differences in tissue growth factor beta 1 (TGFb1)

expression, but TGFb2 was decreased in the SU5416H21/28 group vs. control ($p = 0.04$). There were no significant differences in expression between the groups for tissue growth factor receptor beta 1 (TGFRb1) or TGFRb2.

Discussion

The SU5416/H model was first described by Taraseviciene-Stewart L et al.[1] This model has been used over the years to

perform mechanistic studies of PAH pathogenesis and progression. It has been largely assumed that SU5416 exerts its pharmacologic effect via inhibition of VEGFR. Voelkel and Gomez-Arroyo[12] reviewed the so-called angiogenesis paradox that SU5416-induced VEGFR inhibition combined with hypoxia could produce an angioproliferative/obliterative model of pulmonary hypertension. The paradox was explained by the thesis that an initial wave of EC apoptosis was followed by the emergence of apoptotic-resistant EC proliferation (an expansion of the survivor cells, as it were). It has also been reported that SU5416 via VEGFR blockade causes EC apoptosis followed by expansion of surviving CD34+ cells and transdifferentiation to smooth muscle cells.[13] If SU5416 was functioning solely or primarily in its capacity as a VEGFR inhibitor, then it would follow that other more potent VEGFR inhibitors would also induce PAH when combined with hypoxia. We tested this hypothesis by using cabozantinib, a far more potent and specific VEGFR inhibitor than SU5416. However, whether administered by a single SC injection or by continuous SC infusion, cabozantinib plus hypoxia had only a mild and reversible effect. Although there was sustained severe PAH in the SU5416H model and evidence for pulmonary vascular remodeling as evidenced by the decrease in lumen to media ratio of pulmonary arterioles, there was only a mild reversible increase in RV systolic pressure in the cabozantinib group and no significant pulmonary vascular remodeling at the timepoints studied.

Interestingly, although there was sustained severe pulmonary hypertension in the SU5416 hypoxia-treated groups compared to the cabozantinib hypoxia-treated groups, RVH decreased from days 14 to 28 after removal from hypoxia in the SU5416 group. We hypothesized that this decrease in RV mass might have been due to an increase in RV fibrosis in the SU5416 group at day 28. We observed an increase in RV fibrosis in the SU5416H group starting at day 14, but the extent of fibrosis did not appear sufficient at day 28 to explain an overall decrease in RV mass. We also looked at potential differences in body weights and LV weights between the groups that might represent a confounding variable but this analysis did not explain this unexpected finding. Toba et al.[14] reported a decrease in RVH despite sustained pulmonary hypertension in the SU5416H model at 13 weeks following SU5416 injection. The authors attributed this to the development of RV failure. However, we observed a decrement in RVH at week 7 after the SU5416 injection which seems anomalous. Strain-specific differences as well as differences in response to SU5416 of SD rats from different vendors have been reported.[15] Nevertheless, it seems unlikely that our vendor source of SD rats is sufficient to explain this observation. Further studies in the future may be warranted to confirm or refute this finding.

Kinase inhibitors are often quite permissive, with many "off-target" effects. Kinome screens are standard during development of kinase inhibitors, and many screens are publicly available (lincs.hms.harvard.edu). Not so with SU5416 or cabozantinib. Therefore, we performed a kinome screen of SU5416 (10,000 nM) and cabozantinib (10,000 nM) to identify other possible mechanisms of action for these kinase inhibitors, and we herein provide (to our knowledge) the first reported kinome screens of SU5416 and cabozantinib (Supplemental data). Both SU5416 and cabozantinib were potent against VEGFR2. Somewhat to our surprise, SU5416 also bound with relatively high affinity to BMPR2. Given the binding competition against BMPR2 in the kinome scans, we performed an in vitro BMPR2 activity assay, and confirmed that SU5416 but not cabozantinib inhibited BMPR2. This finding raises the possibility that SU5416 is exerting a pathogenic effect by combined VEGFR/BMPR2 inhibition plus hypoxia. Cabozantinib's high potency against VEGFR2 supports the choice of cabozantinib to test this study's hypothesis.

The Nanostring analyses demonstrated significantly higher gene expression of BMP10 in the SU5416H21/28 group compared to the normal controls. BMP9 and BMP10 are ligands that mediate EC protection and repress chemokine (CC motif) ligand 2 (CCL2) expression, a chemokine involved in monocyte–macrophage recruitment.[16–19] The observed increase in BMP10 in the SU5416H21/28 group suggests a possible counter-regulatory response to perturbation of the BMPR2 axis. These findings suggest important effects of SU5416/hypoxia on the BMPR2 axis that change over time as the model develops. A limitation of this study is that we did not examine BMPR2 expression at earlier timepoints such as during hypoxia exposure or earlier after return to normoxia; thus there may have been alterations of BMPR2 earlier in the development of PH in this model that could have been missed. The increase in VEGFR1 and PDGFB expression in the SU5416H21/28 group vs. control could represent activation of proliferative signaling via these pathways at this timepoint in the SU5416H model. The increase in SMAD9 expression observed in the CaboH21/14 group could represent a counter-regulatory response that might dampen angioproliferative/obliterative vascular signaling. Loss of function SMAD9 mutations have been reported as an infrequent cause of PAH and restoration of SMAD9 functioning could decrease proliferation of PAH smooth muscle cells.[20–22] Sanada et al.[23] recently examined TGF and SMAD levels in human PAH as well as animal models of PAH. By immunofluorescent staining, TGFRb1 was not different in the SU5416H model vs. controls, but TGFRb2 was increased in pulmonary vessels. Western blots of lung lysates actually showed a decrease in TGFRb2/Vinculin. However, gene expression of TGFRb2 was not different in the SU5416H vs. control groups. The gene expression results from Sanada et al.[23] are thus similar to the results of our Nanostring analyses in this regard, and highlight the recognition that changes in gene expression or

absence thereof do not necessarily reflect protein levels and consequent effects on signaling. The apparent discrepancies between changes in protein levels and gene expression also highlight the importance of localized regulation in the microenvironment of pulmonary vascular lesions. Nevertheless, our findings do provide some interesting hypothesis generating observations that warrant further exploration in the future.

Conclusion

Cabozantinib, a potent VEGFR2 inhibitor, plus hypoxia did not induce severe PAH. Severe PAH due to SU5416 plus hypoxia may be due to combined VEGFR2 and BMPR2 inhibition. The modulatory effect of SU5416/hypoxia on the BMPR2 axis in this model represents a new avenue for investigation.

Author contributions

Substantial contributions to the concept or design of the work or the acquisition, analysis, or interpretation of the data: R. Sitapara, C. Sugarragchaa, and L.S. Zisman. Drafting of the work or revising it critically for important intellectual content: R. Sitapara and L.S. Zisman. Final approval for the version submitted: R. Sitapara, C. Sugarragchaa, and L.S. Zisman.

Ethical approval

All research involving animals submitted for publication was approved by an animal care and use committee with oversight of the facility in which the studies were conducted.

Guarantor

Lawrence S. Zisman.

ORCID iD

Lawrence S. Zisman https://orcid.org/0000-0002-7975-4707

References

1. Taraseviciene-Stewart L, Kasahara Y, Alger L, et al. Inhibition of the VEGF receptor 2 combined with chronic hypoxia causes cell death-dependent pulmonary endothelial cell proliferation and severe pulmonary hypertension. *FASEB J* 2001; 15: 427–438.
2. Nicolls MR, Mizuno S, Taraseviciene-Stewart L, et al. New models of pulmonary hypertension based on VEGF receptor blockade-induced endothelial cell apoptosis. *Pulm Circ* 2012; 2: 434–442.
3. Sakao S, Taraseviciene-Stewart L, Lee JD, et al. Vascular endothelial growth factor receptor blockade by SU5416 combined with pulsatile shear stress causes apoptosis and subsequent proliferation of apoptosis-resistant endothelial cells. *Chest* 2005; 128: 610S–611S.
4. Sakao S, Taraseviciene-Stewart L, Lee JD, et al. Initial apoptosis is followed by increased proliferation of apoptosis-resistant endothelial cells. *FASEB J* 2005; 19: 1178–1180.
5. Gross-Goupil M, Francois L, Quivy A, et al. Axitinib: a review of its safety and efficacy in the treatment of adults with advanced renal cell carcinoma. *Clin Med Insights Oncol* 2013; 7: 269–277.
6. Tappenden P, Carroll C, Hamilton J, et al. Cabozantinib and vandetanib for unresectable locally advanced or metastatic medullary thyroid cancer: a systematic review and economic model. *Health Technol Assess* 2019; 23: 1–144.
7. Osanto S and van der Hulle T. Cabozantinib in the treatment of advanced renal cell carcinoma in adults following prior vascular endothelial growth factor targeted therapy: clinical trial evidence and experience. *Ther Adv Urol* 2018; 10: 109–123.
8. Zhang X, Shao Y and Wang K. Incidence and risk of hypertension associated with cabozantinib in cancer patients: a systematic review and meta-analysis. *Expert Rev Clin Pharmacol* 2016; 9: 1109–1115.
9. van Geel RM, Beijnen JH and Schellens JH. Concise drug review: pazopanib and axitinib. *Oncologist* 2012; 17: 1081–1089.
10. Milling RV, Grimm D, Kruger M, et al. Pazopanib, cabozantinib, and vandetanib in the treatment of progressive medullary thyroid cancer with a special focus on the adverse effects on hypertension. *Int J Mol Sci* 2018; 19: 3258.
11. Department of Health and Human Services, Center for Drug Evaluation and Research. Pharmacology/toxicology NDA review and evaluation. *Application number*: 203756.
12. Voelkel NF and Gomez-Arroyo J. The role of vascular endothelial growth factor in pulmonary arterial hypertension. The angiogenesis paradox. *Am J Respir Cell Mol Biol* 2014; 51: 474–484.
13. Sakao S, Taraseviciene-Stewart L, Cool CD, et al. VEGF-R blockade causes endothelial cell apoptosis, expansion of surviving CD34+ precursor cells and transdifferentiation to smooth muscle-like and neuronal-like cells. *FASEB J* 2007; 21: 3640–3652.
14. Toba M, Alzoubi A, O'Neill KD, et al. Temporal hemodynamic and histological progression in Sugen5416/hypoxia/normoxia-exposed pulmonary arterial hypertensive rats. *Am J Physiol Heart Circ Physiol* 2014; 306: H243–H250.
15. Jiang B, Deng Y, Suen C, et al. Marked strain-specific differences in the SU5416 rat model of severe pulmonary arterial hypertension. *Am J Respir Cell Mol Biol* 2016; 54: 461–468.
16. Li W, Long L, Yang X, et al. Circulating BMP9 protects the pulmonary endothelium during inflammation-induced lung injury in mice. *Am J Respir Crit Care Med* . Epub ahead of print 2020. DOI: 10.1164/rccm.202005-1761OC.

17. Long L, Ormiston ML, Yang X, et al. Selective enhancement of endothelial BMPR-II with BMP9 reverses pulmonary arterial hypertension. *Nat Med* 2015; 21: 777–785.

18. Morrell NW. Finding the needle in the haystack: BMP9 and 10 emerge from the genome in pulmonary arterial hypertension. *Eur Respir J* 2019; 53: 1900078.

19. Upton PD, Park JES, De Souza PM, et al. Endothelial protective factors BMP9 and BMP10 inhibit CCL2 release by human vascular endothelial cells. *J Cell Sci* 2020; 133: jcs239715.

20. Drake KM, Dunmore BJ, McNelly LN, et al. Correction of nonsense BMPR2 and SMAD9 mutations by ataluren in pulmonary arterial hypertension. *Am J Respir Cell Mol Biol* 2013; 49: 403–409.

21. Garcia-Rivas G, Jerjes-Sanchez C, Rodriguez D, et al. A systematic review of genetic mutations in pulmonary arterial hypertension. *BMC Med Genet* 2017; 18: 82.

22. Jiang Q, Liu C, Liu S, et al. Dysregulation of BMP9/BMPR2/ SMAD signalling pathway contributes to pulmonary fibrosis and pulmonary hypertension induced by bleomycin in rats. *Br J Pharmacol* 2021; 178: 203–216.

23. Sanada TJ, Sun XQ, Happe C, et al. Altered TGFbeta/SMAD signaling in human and rat models of pulmonary hypertension: an old target needs attention. *Cells* 2021; 10: 84.